

2014

Oxygen vacancy diffusion in bare ZnO nanowires

Bei Deng

Department of Physics and Materials Science, City University of Hong Kong, Hong Kong SAR, China

Andreia Luisa Da Rosa

BCCMS, Universität at Bremen, FB1/NW1, 28359 Bremen, Germany

Th. Frauenheim

BCCMS, Universität at Bremen, FB1/NW1, 28359 Bremen, Germany

J. P. Xiao

BCCMS, Universität at Bremen, FB1/NW1, 28359 Bremen, Germany

X. Q. Shi

Department of Physics, South University of Science and Technology of China, Shenzhen, China

See next page for additional authors

This document is the authors' final version of the published article.

Link to published article: <https://dx.doi.org/10.1039/C4NR03582H>

APA Citation

Deng, B., Da Rosa, A., Frauenheim, T., Xiao, J., Shi, X., Zhang, R., & Van Hove, M. (2014). Oxygen vacancy diffusion in bare ZnO nanowires. *Nanoscale*, 6 (20), 11882-11886. <https://doi.org/10.1039/C4NR03582H>

This Journal Article is brought to you for free and open access by the Research Institutes, Centres and Administrative Units at HKBU Institutional Repository. It has been accepted for inclusion in Institute of Computational and Theoretical Studies by an authorized administrator of HKBU Institutional Repository. For more information, please contact repository@hkbu.edu.hk.

Authors

Bei Deng, Andreia Luisa Da Rosa, Th. Frauenheim, J. P. Xiao, X. Q. Shi, R. Q. Zhang, and Michel Andre Van Hove

ARTICLE

Oxygen vacancy diffusion in bare ZnO nanowires

Bei Deng,^a Andreia Luisa da Rosa,^b Th. Frauenheim,^b J. P. Xiao,^b X. Q. Shi,^c R. Q. Zhang ^{*a} and Michel A. Van Hove.^d

Oxygen vacancies (V_O) are known to be common native defects in zinc oxide (ZnO) and to play important roles in many applications. Based on density functional theory, we present a study for the migration of oxygen vacancies in ultra-thin ZnO nanowires (NWs). We find that under equilibrium growth conditions V_O has a higher formation energy (E_f) inside the wire than at shallow sites and surface sites, with different geometric relaxations and structural reconstructions. The migration of V_O has lower barriers in the NW than in the bulk and is found to be energetically favorable in the direction from bulk to surface. These results imply a higher concentration of V_O at surface sites and also a relative ease of the diffusion in the NW structure. Our results support the previous experimental observations and are important for the development of ZnO-based devices in photocatalysis and optoelectronics.

Introduction

Zinc oxide (ZnO), an important wide band-gap semiconductor, has recently attracted growing attention due to its wide variety of potential applications in optoelectronics, photocatalysis and sensing¹⁻⁴. Although p-type doping of bulk ZnO is still a challenge⁵⁻⁷, it was reported to be possible within nanowire (NW) structures⁸, paving the way to realizing efficient utilization of ZnO as an optoelectronic material for blue and ultraviolet (UV) devices. Besides, enhanced photocatalytic activity of ZnO accompanied by strong defect-related emissions was also demonstrated in NW structures^{9,10}. As a native defect, oxygen vacancies (V_O) are common to exist in ZnO and as such play important roles in many applications. For example, they have been demonstrated to be electron donors responsible for the native n-type character¹¹, and behave as a compensation center for p-type doping¹². The surface of NWs presents significant challenges as well as opportunities for tuning the electronic properties of ZnO. For example, oxygen vacancies have been

suggested to enhance the photocatalytic activity in ZnO NWs, since they can capture photo-generated electrons and holes separately, and play a role in the decomposition of organic contaminants¹³⁻¹⁶ and small molecules¹⁷. Moreover, the V_O defect was also reported to be relevant in the optical emission of ZnO NWs in the visible region^{18,19} and to be responsible for their enhanced photocatalytic activity^{20,21}. Therefore, a detailed understanding of the formation and the migration behavior of the V_O defect in the ZnO NW structure is essential to analyze and optimize the V_O -related properties for ZnO materials.

As V_O normally participates in self-diffusion and impurity diffusion, it is important to understand how these defects migrate in the NW and the impact of the geometric structure on defect migrations. The migration of V_O and other native defects in ZnO bulk crystals has been studied extensively^{22,23}, but knowledge about the migration of V_O in NWs is still limited.

In this work, we theoretically investigate the formation and the migration behavior of V_O in ZnO NWs grown along the [0001] direction, with hexagonal cross sections enclosed by non-polar $\{10\bar{1}0\}$ facets, which is energetically most favorable according to experimental observation^{8,24}. We utilized the Perdew-Burke-Ernzerhof (PBE) functional²⁵ in conjunction with the projected augmented wave²⁶ (PAW) potential to determine the geometries and the charge densities of the defect system. We find that while V_O prefers to be located at surface sites of the wire and has lower migration barriers in ultra-thin NWs than in the bulk, it has even lower migration barrier for moving from the central region toward the surface of the wire rather than from surface to bulk-like sites. Our results may have implication for the development of ZnO-based devices for photocatalysis and optoelectronics.

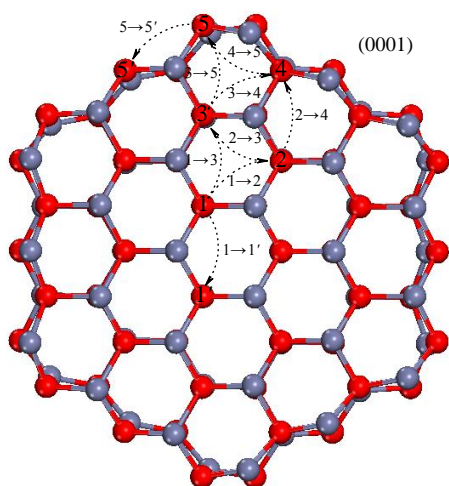


Fig. 1 Axial view of a [0001] ZnO NW. Zn and O atoms are shown in gray and red, respectively. V_O sites (1-5) define possible migration paths along the basal plane.

Computational methods

We performed this study using the density functional theory (DFT), as implemented in the VASP code²⁷, with the generalized gradient approximation (GGA) and the PBE functional. PAW pseudopotentials for the Zn and O were used with a planewave basis set cutoff energy of 500 eV, while Zn

3d states were included in the valence. We used a $1 \times 1 \times 2$ Monkhorst-Pack mesh for the k point sampling in the Brillouin zone. To model the migration behavior of V_O , we set up ZnO NWs enclosed by non-polar $\{10\bar{1}0\}$ facets whose growth is along the [0001] direction consisting of 216 atoms in a repeating slab of 2 double layers with a radius of 16.2 \AA (See the structural model is illustrated in Fig. 1). The migration pathway of the vacancy and the migration energy barrier were determined by finding the minimum energy path from one lattice site to an adjacent site using the nudged elastic band (NEB) method²⁸. A set of intermediate configurations generated by linear interpolation between two endpoint configurations were then optimized. The migration barrier is then given by the energy difference between the equilibrium configurations and the saddle point along the migration path. For an oxygen vacancy in bulk ZnO, we used a $4 \times 4 \times 2$ supercell consisting of 128 atoms with a $2 \times 2 \times 2$ Monkhorst-Pack mesh for the k point samplings, which provides a well converged charge density for the defect system. In all geometric optimizations, all the atoms were allowed to relax until the calculated Hellmann-Feynman forces become smaller than 0.001 eV/\AA .

In thermodynamic equilibrium, the concentration of a defect depends upon its formation energy. In this work, the formation energy of a neutrally charged oxygen vacancy is defined by:

$$E_f = E_{\text{tot}}(\text{ZnO}:V_O) - E_{\text{tot}}(\text{ZnO}) + \mu_O \quad (1)$$

where $E_{\text{tot}}(\text{ZnO}:V_O)$ is the total energy of a NW or bulk sample containing a single, neutral oxygen vacancy, $E_{\text{tot}}(\text{ZnO})$ is the total energy of a perfect ZnO NW or bulk sample, and μ_O is the oxygen chemical potential. The chemical potential depends on the experimental growth conditions and is directly tunable via the change of the relative concentration of O and Zn sources (for example, this can be achieved in MBE or CVD growth). Here we set a lower limit for the oxygen chemical potential: $\mu_O = \mu_{O(O_2)} + \Delta H_f(\text{ZnO})$, corresponding to extreme O-poor conditions. $\Delta H_f(\text{ZnO})$ is the enthalpy of the formation of bulk ZnO and is calculated to be -3.4 eV . It is

possible for the V_O to be charged in p-type samples. However, we expect that the charge density for the positively charged V_O will be delocalized throughout the NW instead of being localized surrounding the defect, due to reconstructions at the surface and sub-surface sites, which are normally absent in bulk-like structure. Thus, cases for the V_O in charged states are more complicated in the NW and this issue needs addressing in the future.

Results and discussion

We obtain a value of 0.73 eV for the formation energy of a single neutral vacancy in ZnO bulk and 0.82 eV for a vacancy in the central region of the wire (Site 1, see Fig. 1). Although traditional density functional methods (GGA or LDA) cannot describe very accurately the formation energy of point defects in solids, migration barriers are obtained as energy differences between electronically similar configurations. Therefore errors in the migration barriers are expected to be smaller than for the formation energies. For instance, Janotti et al.²³ have reported that within the conventional LDA functional, the migration barrier and the activation energy agree very well with the experimental results. Moreover, here we report only changes in the formation energy when the defect diffuses from the central region of the wire to the surface, so that we can exclude the inherent errors calculated within GGA. We find that the formation energy is lowered by 1.14 eV when going from bulk region (Site 1) to a surface site (Site 5), as shown in Fig 2. Compared to the bulk site value, it is lower by 0.05 eV at Site 2, 0.28 eV at Site 3 and 0.47 eV at Site 4. This is consistent with the previous experimental observation¹⁹ that the V_O concentration is the largest near the (10 $\bar{1}$ 0) surfaces of the NWs, and reduces significantly in the interior parts of the NWs. Such differences of formation energy are not surprising. As we will see, at the vicinity of the surface the vacancy has higher freedom to relax while moving, while in the inner part of the NW the relaxation is very similar to the one in the bulk.

Once the vacancy was created in the host, the relaxation of the defect will then take place to minimize the total energy of the system. Because of the surface dependence and the dimensionality difference with crystal bulk, the defect will possess different geometric configurations as occupying different oxygen sites of the

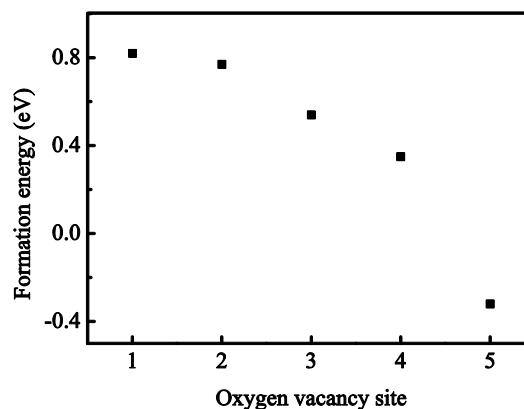


Fig. 2 Formation energy of V_O at different sites of the ZnO NW under Zn-rich conditions

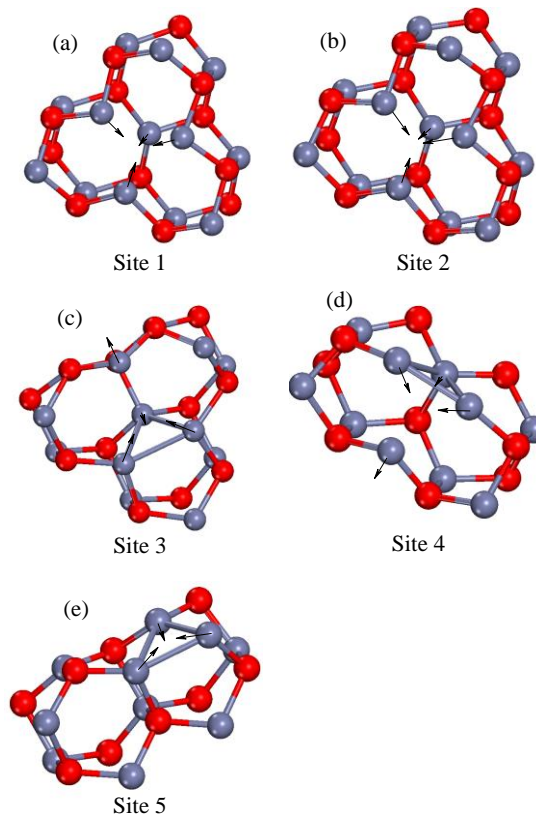


Fig. 3 Local atomic structure of the V_O at (a)-(e) different sites of the ZnO NW, the Zn and O atoms, and the Zn-Zn bonds are indicated by the gray and red spheres, and the gray sticks, respectively.

NW, as shown in Fig 3. At Site1, the four Zn atoms around the vacancy relax inwards and the inward distortion of the Zn atoms is 9.9 % of the Zn-O distance in the absence of V_O . This is consistent with the case in ZnO bulk structure reported in Ref. 23. While at Site 2 (Fig. 3b), the relaxation is less symmetric. Two of the Zn atoms relax inward by 8.4 % and the other two by 13.4%.

Because of the closeness to the surface, vacancies located at Sites 3, 4 and 5 relax differently. At Site 3 one of the Zn atoms adjacent to the vacancy relaxes significantly outwards from the vacancy by 33.1% and the other three move toward the vacancy by 13.4 %, as shown in Fig. 3c. The three nearest Zn atoms will reconstruct and then form long bonds, of which the resulting lengths were obtained to be around 2.74 Å. The defective structure at Site 4 is similar as the one at Site 3, with one Zn atom relaxing outwards and three Zn atoms inwards, as shown in Fig. 3d. The only difference is that the three Zn atoms form even shorter bonds at about 2.70 Å. However, the case is different for site 5, as the removal of the O atom here leaves only three Zn dangling bonds which hybridize and form three Zn-Zn bonds (see Fig. 3e). The resulting bonds are of different lengths which were

calculated to be 2.46, 2.60 and 2.63 Å. It deserves our attention that this reconstruction with symmetry breaking at the surface lowers significantly the energy of the defect system and consequently stabilizes the defective structure.

To further understand the defect formation energy and the associated structural reconstruction in the NW, we next focus on the electronic structure, given in Fig. 4 (a)-(e) for different sites. Note that at relatively deep sites (sites 1 and 2) the $3d$ states of the Zn atoms around the defect remain localized upon the geometric relaxation. This is consistent with the fact that no additional bond is formed when the vacancy is created at these sites. However, the neighboring Zn $3d$ states become somewhat broader when the defect is located at shallower sites (Sites 3 and 4), the broadened DOS in Fig 4 (c)-(d) evidences the close interaction of the Zn-Zn atoms which is responsible for the lower formation energy. Note also that the corresponding $3d$ states become even more broader at Site 5, suggesting that Zn-Zn interaction is stronger at the surface and may be the driving force for the energetically favorable structure obtained at the surface of the NW.

Having established the defect structure of V_O in the ZnO NW, we next examine several migration paths for the oxygen vacancy between nearest neighbors, as depicted in Fig. 1. Migration barriers between second nearest vacancies have been reported to be much higher than that between nearest neighbors in ZnO bulk²⁹. As previously suggested by Anderson *et al.*²³ the migration of V_O is almost isotropic in bulk ZnO, and therefore we consider here only the migration of V_O in the basal plane. For comparison we have also calculated the migration barrier of V_O in ZnO bulk.

The energy curves along the migration path of V_O in a NW are shown in Fig. 5a, where the configuration coordinate is indicated as the distance between the position of the vacancy along the path and its initial position. The obtained barrier for migration of V_O in the bulk is 2.35 eV and is well consistent with previous DFT results²³. As can be seen from Fig. 5a, the migration barriers for V_O are lower in the NW than in the bulk, even for the central sites. Specifically, the

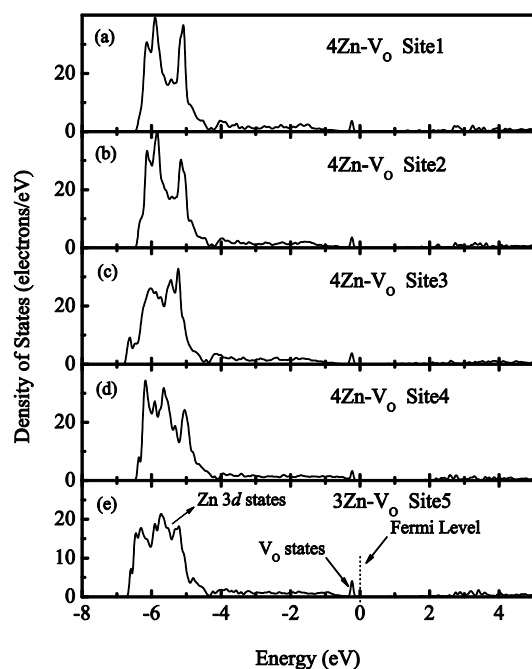


Fig. 4. (a)-(e) The projected density of states (PDOS) for V_O and the neighboring Zn at Sites 1-5 of the ZnO NW

obtained barriers are 1.74, 1.31 and 1.48 eV for transitions 1→2, 1→3 and 2→3, respectively. For shallower sites, the migration barriers are obtained to be even smaller, namely, 1.57, 1.32, 1.01 and 1.43 eV for transitions 2→4, 3→4, 3→5 and 4→5, respectively. The reason that migration barriers for V_O are lowered and have different values in the NW can be qualitatively understood as follows: i) the saddle-point configurations for migration of the vacancy normally correspond to a large distortion of the local atomic arrangement. In the NW structure since the wire is surrounded by vacuum (under ambient conditions perhaps the surface

dangling bonds would be saturated), the geometric structure can relax more freely in the basal direction; ii) the V_O defect has different formation energies and different thermal stabilities in the NW as discussed above, leading to different shapes of the potential energy surface along the migration path and thus different barriers for migration.

Migration barriers of the V_O defect should be different for NWs of different sizes. To verify this, we have set up a thinner wire with a radius of 9.7\AA . The obtained barriers within this wire are 1.05 eV for transition 3→5 and 1.59 eV for 3→4. Note that the barriers are increased as the size of the NW is reduced, which is especially true for transition 3→4. This is because: on one hand, the smaller wire has a higher ratio of surface unsaturated bonds versus internal bonds, leading to higher bonding strength for the latter, and this will consequently increase the barrier for V_O diffusion; On the other hand, the smaller wire possesses a lower rigidity of the lattice³⁰ and thus can relax more freely, and this will lower the barrier for V_O diffusion. As a net result, the migration barriers are different for migrations in NWs with different sizes. It is important to point out that for some ultra-large-size wires the transition barriers should be values as large as the one in the bulk, since the atomic configuration and the defect structure become approximately bulk-like. Therefore, the diffusion of V_O in the NW is size-dependent and there must be a size value for the wire that is most favorable for the defect diffusion. Due to restriction of the computational capability, here we do not discuss more for this issue, and further effort should be paid in this direction.

Note that the migration behavior of V_O also has another tendency in the NW, i.e., the calculated barrier is 1.31 eV for transition 1→3 compared with 1.55 eV for its reverse transition 3→1, and 1.01 eV for 3→5 compared with 1.88 eV for 5→3 (see Fig. 5a). These results demonstrate that the V_O migration is more likely to happen following the bulk→surface direction, as diffusions from inner sites to outer sites always have lower barriers compared to their reverse transitions. Because the energy minima along the potential energy curve are deeper at the surface and sub-surface sites

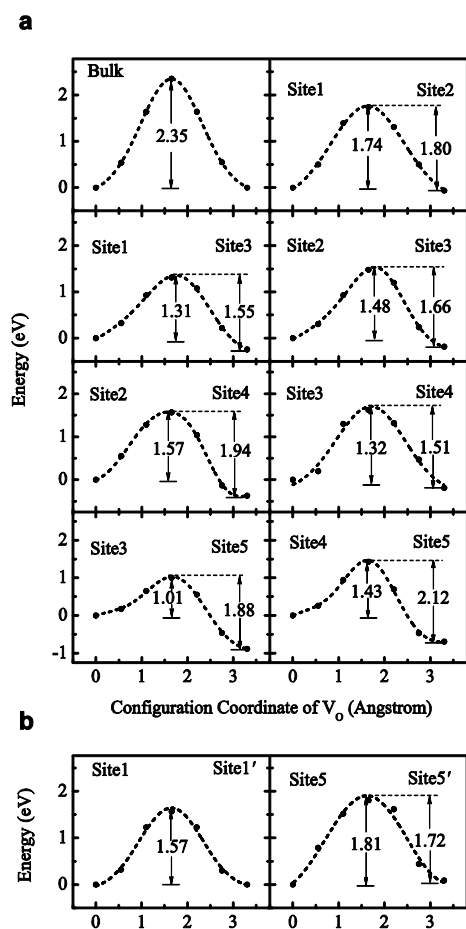


Fig. 5. a) Potential energy of V_O along the migration path between different sites of the ZnO NW; the calculated energy curve in bulk ZnO is given in the top left panel. b) Potential energy of V_O along the migration path between equivalent sites of the ZnO NW. Dots are calculated result, while dashed lines are fitted polynomials.

than in the center of the NW, the defect will preferably migrate toward the surface direction. This can be understood also as a staged decline of the potential energy along the bulk→surface direction, which is consistent with the decreased formation energy obtained in Fig 2. Note that the decline is particularly steep along the $[22\bar{1}0]$ direction (1→3→5), indicating a most favorable path for the V_O diffusion in ZnO NW. In addition, here we give the energy curves and the migration barriers of V_O between two equivalent sites at bulk and surface, i.e. 1→1' and 5→5' (see Fig. 1). The energy curves are shown in Fig. 5b and the obtained barriers are 1.57 and 1.81 eV for paths 1→1' and 5→5' respectively, which suggests that the defect becomes less movable once located at the surface. The relatively higher barrier obtained for the diffusion between surface sites is due to Zn-Zn bond breaking at the initial stage which requires larger energy.

Summary and conclusions

In conclusion, based on our calculations and in agreement with experimental observation, V_O defects favor migration toward the surface of ZnO NWs, due to lowered formation energy and accompanied by associated structural relaxation or reconstructions. The migration barriers reveal easier diffusion of V_O in NWs compared to bulk ZnO. These results suggest a higher concentration of V_O at surface and shallow sub-surface sites compared to the inner sites of the NW, and therefore provide a possible explanation for the enhanced photocatalytic activities in ZnO NWs observed in Ref. 14. our results show that migration of V_O from inner sites to the surface are more favorable than the reverse paths. This could lead to a pathway for successful p-type doping where the impurity could diffuse to inner sites of the NW with the mediation of V_O , leaving the vacancy at the surface and suppressing the V_O -related compensation for p-type doping. Beyond this specific application, the NW structure of ZnO may also prove to be useful as a means to optimize or control defect-related properties for numerous potential applications

in optoelectronics and photocatalysis.

Acknowledgements

The work described in this paper is supported by grants from the Research Grants Council of Hong Kong SAR [Project Nos. CityU 103913], the Deutsche Forschungsgemeinschaft under the program FOR1616, and the Deutsche Akademische Austausch Dienst under the exchange program Germany-Hong Kong. MAVH was supported by the HKBU Strategic Development Fund.

Notes and references

^aDepartment of Physics and Materials Science, City University of Hong Kong, Hong Kong SAR. Email: aprqz@cityu.edu.hk

^bBCCMS, Universität Bremen, FB1/NW1, 28359 Bremen, Germany

^cDepartment of physics, South University of Science and Technology of China, Shenzhen, China.

^dInstitute of Computational and Theoretical Studies and Department of Physics, Hong Kong Baptist University, Hong Kong SAR

¹ M. Li, G. C. Xing, G. Z. Xing, B. Wu, T. Wu, X. H. Zhang, and T. C. Sum, Phys. Rev. B **87**, 115309 (2013).

² M. Kong, Y. Z. Li, X. Chen, T. T. Tian, P. F. Fang, F. Zheng, and X. J. Zhao, J. Am. Chem. Soc. **133**, 16414 (2011).

³ Y. F. Hsu, Y. Y. Xi, A. B. Djurisic, and W. K. Chan, Appl. Phys. Lett. **92**, 133507 (2008).

⁴ Y. Zhang, R. E. Russo, and S. S. Mao, Appl. Phys. Lett. **87**, 043106 (2005).

⁵ B. Deng, Z. Y. Guo, and H. Q. Sun, Appl. Phys. Lett. **96**, 172106 (2010).

⁶ J. Li, S.-H. Wei, S.-S. Li and J.-B. Xia, Phys. Rev. B **74**, 081201(R) (2006).

⁷ S. Limpijumngong, S. B. Zhang, S.-H. Wei, and C. H. Park, Phys. Rev. Lett. **92**, 155504 (2004).

⁸ B. Xiang, P. Wang, X. Zhang, S. A. Dayeh, D. P. R. Aplin, C. Soci, D. Yu, and D. Wang, Nano Lett. **7**, 323 (2007).

⁹ Q. Wan, T. H. Wang, and J. C. Zhao, Appl. Phys. Lett. **87**, 083105 (2005).

¹⁰ Y. H. Zheng, L. R. Zheng, Y. Y. Zhan, X. Y. Lin, Q. Zheng,

- and K. M. Wei, *Inorg. Chem.* **46**, 6980 (2007).
- ¹¹S. B. Zhang, S.-H. Wei, and A. Zunger, *Phys. Rev. B* **63**, 075205 (2001).
- ¹²Y. Yan, S. B. Zhang, and S. T. Pantelides, *Phys. Rev. Lett.* **86**, 5723 (2001).
- ¹³T. J. Kuo, C. N. Lin, C. L. Kuo, and M. H. Huang, *Chem. Mater.* **19**, 5143 (2007).
- ¹⁴F. Xu, Y. T. Shen, L. T. Sun, H. B. Zeng, Y. N. Lu, *Nanoscale* **3**, 5020 (2011).
- ¹⁵Q. Wan, T. H. Wang, and J. C. Zhao, *Appl. Phys. Lett.* **87**, 083105 (2005).
- ¹⁶Y. H. Zheng, L. R. Zheng, Y. Y. Zhan, X. Y. Lin, Q. Zheng, and K. M. Wei, *Inorg. Chem.* **46**, 6980 (2007).
- ¹⁷M. J. Spencer, K. W. Wong and I. Yarovsky, *J. Phys.: Condens. Matter* **24**, 305001 (2012).
- ¹⁸R. M. Sheetz, I. Ponomareva, E. Richter, A. N. Andriotis and M. Menon, *Phys. Rev. B* **80**, 195314 (2009).
- ¹⁹K. M. Wong, S. M. Alay-e-Abbas, Y. G. Fang, A. Shaikat and Y. Lei, *J. Appl. Phys.* **114**, 034901 (2013)
- ²⁰G. Y. Huang, C. Y. Wang and J. T. Wang, *J. Appl. Phys.* **105**, 073504 (2009).
- ²¹K. E. Knutsen, K. M. Johansen, P. T. Neuvonen, B. G. Svensson and A. Yu. Kuznetsov, *J. Appl. Phys.* **113**, 023702 (2013).
- ²²G. Neumann, in *Current Topics in Materials Science*, edited by E. Kaldis (North-Holland, Amsterdam, 1981), Vol. 7, p. 279.
- ²³A. Janotti and C. G. Van de Walle, *Phys. Rev. B* **76**, 165202 (2007).
- ²⁴C. H. Liu, W. C. Yiu, F. C. K. Au, J. X. Ding, C. S. Lee, and S. T. Lee, *Appl. Phys. Lett.* **83**, 3168 (2003).
- ²⁵J. P. Perdew, k. Burke and M. Ernzerhof, *Phys. Rev. Lett.* **77**, 3865 (1996).
- ²⁶G. Kresse and D. Joubert, *Phys. Rev. B* **59**, 1758 (1999).
- ²⁷G. Kresse and J. Furthmuller, *Phys. Rev. B* **54**, 11169 (1996).
- ²⁸H. Jonsson, G. Mills and K. W. Jacobsen, "Nudged Elastic Band Method for Finding Minimum Energy Paths of Transitions", in "Classical and Quantum Dynamics in Condensed Phase Simulations", ed. B. J. Berne, G. Ciccotti and D. F. Coker (World Scientific, 1998).
- ²⁹P. Erhart and K. Albe, *Phys. Rev. B* **73** 115207 (2006).
- ³⁰D. K. Yu, R. Q. Zhang, and S. T. Lee *Phys. Rev. B* **65**, 245417 (2002)